A CRACK GROWTH MODEL UNDER SPECTRUM LOADING

ICAS-82-2.5.4

Yang Bing-Xian

Beijing Institute of Aeronautics and Astronautics

Beijing, the People's Republic of China

Abstract

In the present study, based on the mechanisms of delayed retardation of overload retardation effect, an analytical equation for predicting the delayed retardation parameter is presented. Further, a model for predicting the retardation under tensile overloads and tensile-compressive overloads is proposed, and it can be used to predict the fatigue crack growth rate and fatigue life under complex spectrum loading. And as an example, the retardation effects of some materials under different loading conditions are predicted. The fatigue life of stiffened panel of wing and landing gear of aircraft under complex spectrum loadings are predicted. Predictions agree very well with experimental results.

I. Introduction

The simplest case for the spectram loading is that where a single or multiple tensile and tensile-compressive overloads are applied to a constant amplitude cyclic loading. After the application of the overloads, the crack growth at a lower rate than it did prior to the application of the overload. It is well known that the minimum growth rate did not occur immediatly after the application of the overload cycle, but it is reached only after the crack has grown a small distance a_{min} . This phenomenon is referred to as delayed retardation. Previous models on retardation predictions, such as Elber, Wheeler, Willenhorg models, did not take account of the effect of delayed retardation. Therefore, the predictions of crack growth rate and fatigue life by those models did not always agree with experimental results.

Matsuoka model[1] has taken account of the effect of delayed retardation. The retarded crack growth rate can be calculated by the following equation as proposed by Matsuoka

$$\left(\frac{da}{dN}\right)_D = U_D^n \left(\frac{da}{dN}\right)_C \qquad (1)$$

where $\left(\frac{da}{dN}\right)_C = C\,(\Delta K_1)^n$ is the fatigue crack growth rate under constant amplitude cyclic loading :

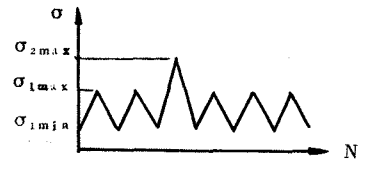

Fig. 1 Single overload pattern

and $\Delta k_1 = (\sigma_{1max} - \sigma_{1min})\sqrt{\pi a}$ is the stress intensity factor range (Fig.1) c,n are Empirical constants of the Paris equation[1].

$$U_D = 1-\left(\frac{r}{2}\right)\left(\frac{a^*}{a_{min}}-1\right)(a-a_o)/a^*$$

$$0 \le a-a_o \le a_{min}$$

$$U_D = 1-\left(\frac{r}{2}\right)\left[1-\frac{a-a_o}{a^*}\right], \quad a_{min} \le a-a_o \le a^* \qquad (2)$$

where a^* is the overload affected zone size,

a_{min} is the crack distance at the maximum retardation from the point of application of overload.

$r = \Delta\sigma_2/\Delta\sigma_1$ is the overload ratio, namely the ratio of peak stress range to baseline stress range,

a is the current crack length,

a_o is the crack length at the point of application of overload. (Fig.2)

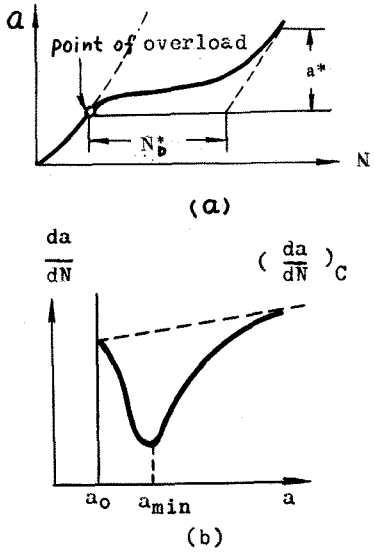

Fig.2 Schematic illustration of delaged phenomenon.

Equation (1) and (2) indicate that the crack growth rate during retardation is expressed as a function of the ratio, r, the overload affected zone size, a^*, the crack distance at the maximum retardation from the point of application overload, a_{min} , and the exponent parameter of the material, n.

References (2) (3) evaluated by comparisions all previous models both theoretically and experi-

mentally, and pointed out that the Matsuoka model is the best one. But the important parameter a_{min} in Matsuoka model had to be determind only by experiments, so the prediction of fatigue lifes of structures is very inconvenient.

In the present study, based on the mechanisms of delayed retardation, an analytical equation for predicting the parameter a_{min} is proposed. Further, this paper proposed a model for predicting the retardation under tensile overloads, tensile-compressive overloads and compressive-tensile overloads. Using this model, we can predict the fatigue crack growth life of structures under complex spectrum loadings.

II. Determination of the parameter a_{min}

How do we explain the delayed retardation phenomenon? It is because of (1) crack blunting induced by the large deformation due to the overload cancels the closing force due to the residual strain left by the overload. (2) During the overloading, the crack growth accelerate and after overloading, it still has acceleration effect.

Kobayashi et al[4] have studied the fatigue crack growth acceleration during a single peak overloading and after it. Electron microfractographic studies have shown that the stretched zone width, SZW, induced by the overload, is much larger than the variations of striation spacings, s, formed by the constant stress. It shown that there is obvious acceleration during the overload. After the overload, due to the effect of previous acceleration, there still exists initial acceleration.

On the other hand, the geometric blunting of the crack tip due to the application of the overload tends to open up the crack tip and will cancel the closing force. Thus, the effects of the initial acceleration and blunting of crack tip delay the occurrence of the maximum retardation up to the distance a_{min}. Therefore, the associating crack growth rate will decrease gradually in the early stage of retardation before its minimum value is reached, and then it turn to increase with decrease in the remaining zone-size of the residual compressive stress ahead of the crack tip.

Miyamoto et al[5] have calculated the stress distributions after the application of overload for the material with the strain hardening behavior $H'/E=1/400$ by the finite element method. It shows that the maximum residual compressive stress is reached after a small distance from the point of application of overload.

Keiji Ogura et al[6] obtained the same conclusions, that various H'/E values only affect the values of residual compressive stress, while the distribution trends are identical. These results verified also that the delayed retardation really exists for different materials.

In the present studies, several tests were performed using different overload ratios. The material used was LY-12. The measurement of crack growth was conducted on specimens of 2.2mm thick and 100mm wide plates with a 6mm-dia. central hole and 4mm long saw cuts. Fractographic examinations were conducted. There is a dard band at the position where the overload has been applicated as shown in Fig.(3) . The greater the overload, the more distinct the dark band well be, and it is larger at the inter part than at the outer part of the specimen.

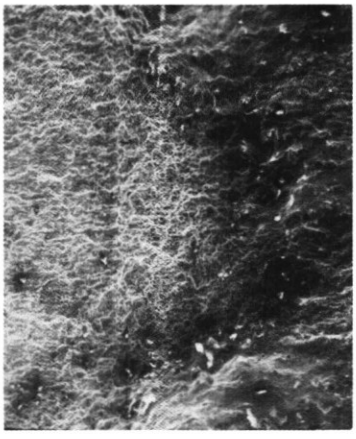

crack growth direction
(a)

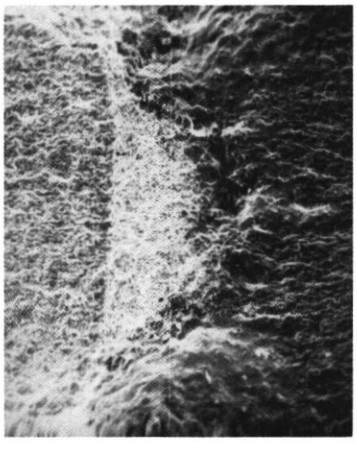

crack growth direction
(b)

Fig.3 Fractograph (a) r=1.8
(b) r=2.0

From the fractographs, we may observed a stretched zone and followed by abrasion surface. Such fractographic features are analogous to other metallic materials. We also observed that immediately the application of overload, the crack tip remained open even at the unloading state.

Based on the crack growth mechanisms before and after overloading as mentioned above, we may suggest that after the peak overload there is an overload affected zone, and in which two important factors act simultaneously. One of them is the closing of the crack tip by the re-

sidual plastic strain, the other one is the opening of the crack tip by blunting. These two opposite factors may operate more or less at the tip of a crack propagating steadily under constant amplitude loading. But during the initial stage of retardation in certain crack distance from the point of application of overload, the blunting of crack tip is the main affecting factor whill the closing of the crack tip is secondary affecting factor. Thus we may name the distance a_{min} as "the blunting affected zone", in which delayed retardation is produced by the resultant of the effect of the two factors. Beyond the blunting effected zone, the closing of the crack tip becomes the main affecting factor.

The question is how to determine the blunting affected zone size, a_{min}, by the analytical method.

Based on the mechanism of crack tip blunting, the order of blunting may be represented by the crack tip opening displacement, CTOD, or by the crack extension, Δa. In the case of linear elastic range, after peak overload, CTOD is given by the following expression

$$(CTOD)_{2max} = \frac{K^2_{2\,max}}{\lambda E \sigma_{ys}} \tag{3}$$

In the case of elastic-plastic range, it may be discribed by the J-integral

$$CTOD = \frac{J}{\lambda \sigma_{ys}} \tag{4}$$

As taking account of the strain hardening,

$$CTOD = \frac{J}{\lambda \sigma_{flow}} \tag{5}$$

The relation between the crack extension and the crack opening displacement is given as

$$\Delta a = \frac{1}{2} CTOD$$

The stretched zone width after the application of peak overload is just the result from crack tip plastic blunting. The relation between the SZW and the CTOD is

$$SZW = \frac{1}{4} (CTOD)_{2max} \tag{6}$$

thus

$$SZW = \frac{1}{4} \frac{K^2_{2max}}{\lambda E \sigma_{ys}} = \gamma \frac{\sigma_{ys}}{E} R^P_{YR} \tag{7}$$

where σ_{ys} is the yield stress

E is Young's modulus

R^P_{YR} is the size of residual plastic zone size left by peak stress.

Blunting affected zone size is propertional to the stretched zone size, and may be discribed as

$$a_{min} = \beta (SZW)$$

or

$$a_{min} = \beta \frac{\sigma_{ys}}{E} R^P_{YR} \tag{8}$$

Based on the experimental and statistical results $\beta = 120\text{-}140$ for all metallic materials. Taking $\beta = 130$, we obtain the following simple expression for predicting the delayed retardation parameter, a_{min},

$$a_{min} = 130 \frac{\sigma_{ys}}{E} R^P_{YR} \tag{9}$$

where

$$R^P_{YR} = \frac{1}{\pi} \left(\frac{\Delta K_2}{2\sigma_{ys}}\right)^2 = \frac{1}{\pi} \left(\frac{\Gamma \Delta K_1}{2\sigma_{ys}}\right)^2 \tag{10}$$

Equations (9) and (10) indicate that a_{min} is described as a function of the baseline cyclic stress intensity factor range, ΔK_1, overload ratio, r, and material constants σ_{ys} and E. Therefore when the overload ratio and material's constants are given, a_{min} can be obtained simply.

In this paper, the values of a_{min} for HT80 steel, A553 steel, A5083 aluminum alloy, LY-12 aliminum alloy and Ti-6Al-4V titanium alloy under different loading conditions are predicted. The predictions agree very well with experimental results.

III. Evaluations of U_D, $(\frac{da}{dN})_D$ and N_D

After obtaining the value of a_{min}, we can predict the value of U_{Dmin}

$$U_{Dmin} = 1 - \frac{r}{2}\left(1 - \frac{a_{min}}{a^*}\right) \tag{11}$$

Since the value of U_D is varying linearly with a, then it can be obtained from the diagram very simply as shown in Fig. 4. The expresions of two linear parts are discribed as

$$U_D = 1 - \frac{r}{2}\left(\frac{a^*}{a_{min}} - 1\right)\frac{a}{a^*} \quad \text{for } 0 \le a \le a_{min}$$

$$U_D = 1 - \frac{r}{2}\left(1 - \frac{a}{a^*}\right) \quad \text{for } a_{min} \le a \le a^* \tag{12}$$

$$\left(\frac{da}{dN}\right)_{min} = U^n_{Dmin} \left(\frac{da}{dN}\right)_C \tag{13}$$

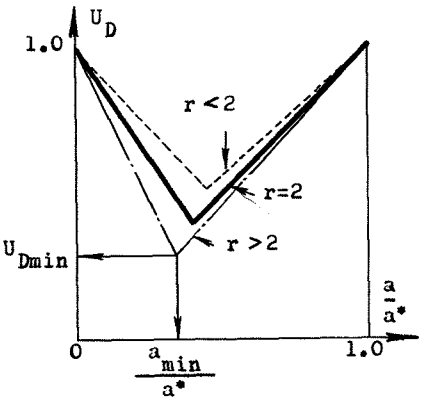

Fig. 4 diagram for finding U_D

The retardation N_D can be obtained by integrating equation (1) as follows

$$N_{D1} = \int_0^{a_{min}} \frac{da}{U_D^n \left(\frac{da}{dN}\right)_C} = \frac{1}{\left(\frac{da}{dN}\right)_C} \int_0^{a_{min}} U_D^{-n}\, da$$

$$= \frac{1}{(\frac{da}{dN})_c} \int_0^{a_{min}} \left[1 - \frac{r}{2}\left(\frac{a^*}{a_{min}} - 1\right)\frac{a}{a^*}\right]^{-n} da$$

$$= \frac{a^*}{(\frac{da}{dN})_c} \cdot \frac{(U_{Dmin})^{1-n} - 1}{\frac{r}{2}(\frac{a^*}{a_{min}} - 1)(n-1)} \qquad (14)$$

$$N_{D2} = \int_{a_{min}}^{a^*} \frac{da}{U_D(\frac{da}{dN})_c} = \frac{1}{(\frac{da}{dN})_c} \int_{a_{min}}^{a^*} U_D^{-n}\, da$$

$$= \frac{1}{(\frac{da}{dN})_c} \int_{a_{min}}^{a^*} \left[1 - \frac{r}{2}\left(1 - \frac{a}{a^*}\right)\right]^{-n} da$$

$$= \frac{a^*}{(\frac{da}{dN})_c} \cdot \frac{(U_{Dmin})^{1-n} - 1}{\frac{r}{2}(n-1)} \qquad (15)$$

The total number of cycles of retardation N_D, is

$$N_D = N_{D1} + N_{D2}$$

$$N_D = \frac{a^*}{(\frac{da}{dN})_c} \cdot \frac{(U_{Dmin})^{1-n} - 1}{\frac{r}{2}(1 - \frac{a_{min}}{a^*})(n-1)} \qquad (16)$$

The overload affected zone size, a^*, is expressed as

$$a^* = \left[2.5\left(\frac{r}{2}\right)^2 - \frac{1}{2}\left(\frac{1}{1-R}\right)^2\right] R_{y_o} \qquad (17)$$

where R_{y_o} is the monotonic plastic zone size produced by the loading of baseline stress intensity factor, ΔK_1.

The curves of crack growth rate versus the crack length and the curves of crack length versus number of cycles during retardations are plotted in Fig. 5 - Fig. 8 for A5083 Al and HT80 steel respectively.

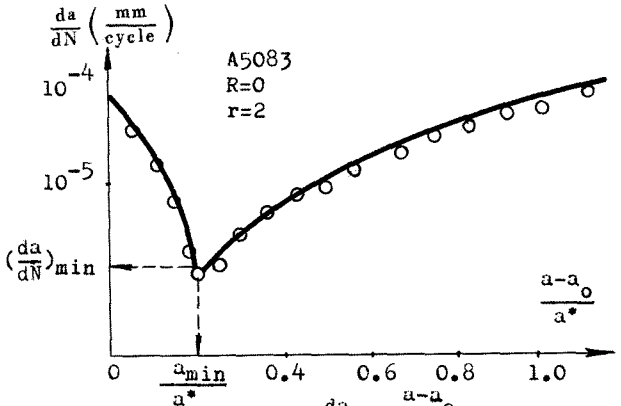

Fig. 5 A5083 Al, $\frac{da}{dN}$ vs $\frac{a-a_o}{a^*}$ curve during retardation

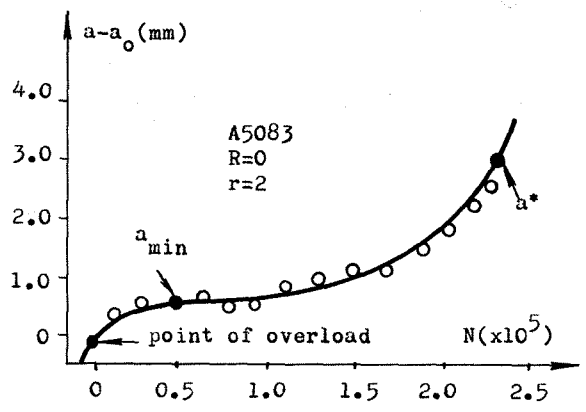

Fig. 6 A5083 Al, $(a-a_o)$ vs N curve during retardation

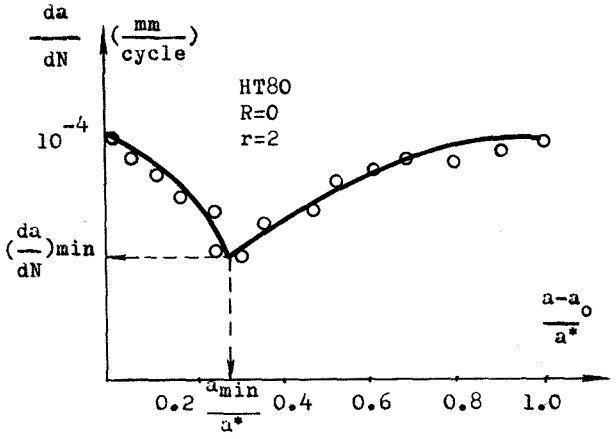

Fig. 7 HT80 steel. $\frac{da}{dN}$ vs $\frac{a-a_o}{a^*}$ curve during retardation

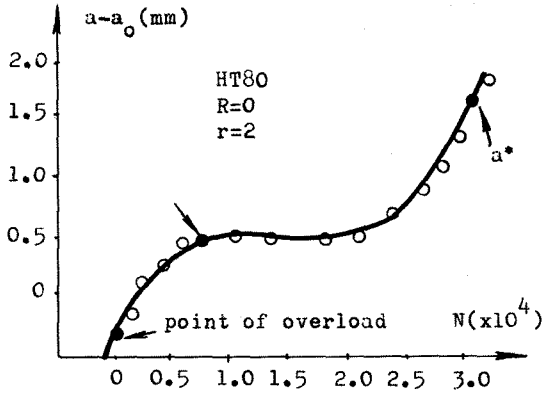

Fig. 8 HT80 steel $(a-a_o)$ vs N curve during retardation

TABLE 1 COMPARISONS BETWEEN THE CALCULATIONS AND EXPERIMENTS UNDER TENSILE OVERLOAD

material	t (mm)	w (mm)	K_1 ($\frac{kg}{mm^{3/2}}$)	R	r	$\frac{a_{min}}{R^o_{YR}}$		$\frac{a_{min}}{a^*}$		$\frac{(da/dN)_{min}}{(da/dN)_o}$		N_D (cycle)	
						cal.	exper.	cal.	exper.	cal.	exper.	cal.	exper.
HT80	4.0	120	133	0	2	0.486	0.47	0.30	0.29	0.087	0.083	32000	29000 (10)
A533	3.5	120	96.6	0	2	0.47	0.48	0.19	0.20	0.037	0.038	59000	63000 (10)
A5083	8.0	120	33.8	0	2	0.27	0.30	0.194	0.20	0.0095	0.014	222000	225000(10)
2024-T3	3.22	76.2	63.7	0.05	1.75	0.68		0.266	0.25	0.055		12800	9500(11)
LY-12	4.0	100	31	0.1	2	0.625		0.31		0.011		329000	32000
Ti-6Al-4V	5.0	120	92.4	0	2	1.24	1.28	0.31	0.32	0.03	0.038	13300	11500(10)

Table 1 listed the experimental and calculated results of a_{min}/R^P_{YR}, a_{min}/a^*, $(\frac{da}{dN})_{min}$, N_D, for HT80 steel, A533 steel, A5083Al, A2017Al, 2024-T3 Al, LY-12Al and Ti-6Al-4V.

Fig. 5-8 and Table 1. Show that the experimental results fit excellently with the predicted results by the present method.

IV. The influence of compressive overload

We consider two cases, in the first case, after a tensile overload followed by a compressive overload (case T-C) and in the second case, after a compressive overload followed by a tensile overload (case C-T), the following parameters are introduced.

overload ratio $r = \dfrac{\sigma_{2max}-\sigma_{1min}}{\sigma_{1max}-\sigma_{1min}}$

baseline cyclic stress ratio $R = \dfrac{\sigma_{1min}}{\sigma_{1max}}$

overload stress ratio $R_{o1} = \dfrac{\sigma_{2min}}{\sigma_{2max}}$

overload stress range ratio

$$\Delta R_{o1} = \frac{\sigma_{2min}-\sigma_{1min}}{\sigma_{2max}-\sigma_{1min}}$$

For the case T-C, the stress distribution of the crack tip can be obtained also by the Rice's superposition method. It may be reasonable to assume that after the crack blunting induced by the large deformation due to the tensile overload, the crack tip do not close even after the compressive overload is applied, and that the stress intensity factor range ΔK_2 has full attribution to produce plastic zone, then the cyclic plastic zone size produced by the overload becomes

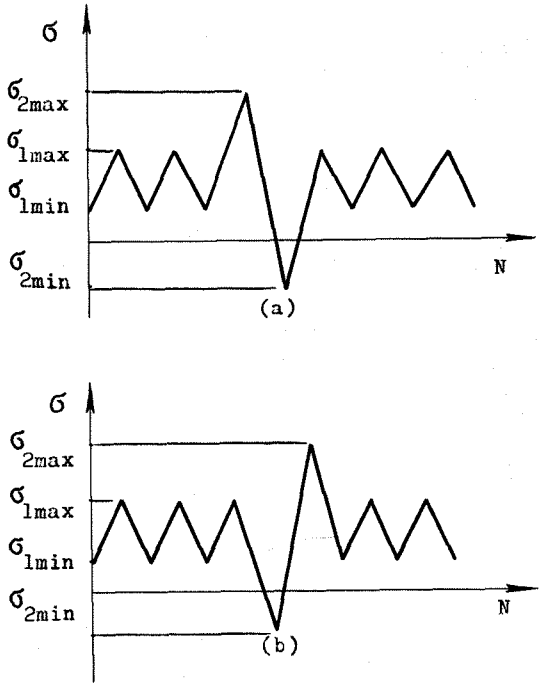

Fig. 9 Definition of compressive overload terminology

$$R^P_{yR} = \frac{1}{\pi}\left(\frac{\Delta K_2}{2\sigma_{ys}}\right)^2 \tag{18}$$

$$\Delta K_2 = Y\left(1-\Delta R_{o1}\right)\Delta K_1 \tag{19}$$

$$R^P_{yR} = \left(\frac{Y}{2}\right)^2\left(1-\Delta R_{o1}\right)^2 R_{yo}$$

where $R_{yo} = \frac{1}{\pi}\left(\frac{\Delta K_1}{\sigma_{ys}}\right)^2$

There is residual tensile stress in the residual stress produced by the compressive overload unloading, it relaxes the residual compressive stress produced by the tensile overload. The stress intensity factor range ΔK_1 after compressive overload becomes

$$\Delta K_1' = K_{1max} - K_{2min} = (1 - r\Delta R_{ol})\Delta K_1 \qquad (20)$$

and the cyclic plastic zone size produced by $\Delta K_1'$ is

$$R_{yR}^c = \frac{1}{\pi}\left[\frac{(1 - r\Delta R_{ol})\Delta K_1}{2\sigma_{ys}}\right]^2 = \left[\frac{(1 - r\Delta R_{ol})}{2}\right]^2 R_{yo} \qquad (21)$$

So that the relation between the two plastic zones after tensile-compressive overload is as follows

$$\frac{R_{yR}^c}{R_{yR}^P} = \frac{\left[\frac{1}{2}(1 - r\Delta R)\right]^2}{\left[\frac{r}{2}(1 - \Delta R)\right]^2} = \frac{(1 - r\Delta R_{ol})^2}{r^2(1 - \Delta R_{ol})^2} \qquad (22)$$

But when only the tensile overload (case T) is applied, the relation between plastic zones is as follows.

$$\frac{R_{yR}^c}{R_{yR}^P} = \frac{(\frac{1}{2})^2 R_{yo}}{(\frac{r}{2})^2 R_{yo}} = \frac{1}{r^2} \qquad (23)$$

Taking r=2, R_{ol}=-0.5 and substituting them into Eq. (22) gives

$$\frac{R_{yR}^c}{R_{yR}^P} = \left(\frac{1}{1.5}\right)^2$$

It shows that, the case r=2, ΔR_{ol}=-0.5, under the tensile-compressive overloading is equivalent to the case r=1.5 , under the tensile overloading Namely the retardation effect after the tensile-compressive overload is equivalent to a tensile overload case with σ_{1min} dropping down to σ_{2min} and an overload ratio r'.

$$r' = \frac{\Delta K_2}{\Delta K_1} = \frac{K_{2max} - K_{2min}}{K_{1max} - K_{1min}} = \frac{r(1 - \Delta R_{ol})}{1 - r\Delta R_{ol}} \qquad (24)$$

Therefore, in the case of tensile-compressive overload the tensile overload model can also be used, but the overload ratio r should be replaced by it's equivalent value r'.

For the case of compressive overload followed immediatly by the tensile overload (case C-T), since the compressive overload cannot cause the crack blunting and almost does not affect the stress distribution at crack tip, it is equivalent to that σ_{2min} rises up to σ_{1min} level, as well as R_{ol}=0, r'=r, namely the case C-T is almost identical to the case T.

The comparisons between the calculated and experimental results are listed in table 2 for the case of T-C.

TABLE 2 COMPARISONS BETWEEN THE CALCULATIONS AND EXPERIMENTS UNDER TENSILE-COMPRESSIVE LOAD

material	t (mm)	w (mm)	K_1 ($\frac{kg}{mm^{3/2}}$)	R	r	R_{ol}	$\frac{a_{min}}{a^*}$ cal.	$\frac{a_{min}}{a^*}$ exper.	$\frac{(da/dN)_{min}}{(da/dN)_c}$ cal.	$\frac{(da/dN)_{min}}{(da/dN)_c}$ exper.	N_D (cycle) cal.	N_D (cycle) exper.	
HT80	4	140	133	0	2	0	0.30	0.29	0.087	0.087	32000	29000	(10)
	4	140	133	0	2	-0.25	0.336	0.331	0.199	0.192	26000	25000	
	4	140	133	0	2	-0.5	0.46	0.39	0.348	0.204	17800	17500	
	4	140	133	0	2	-1.0	0.439	0.41	0.39	0.369	14800	15500	
A5083	8	140	28	0	2	0	0.19	0.22	0.01	0.015	215000	250000	(10)
	8	140	28	0	2	-0.25	0.21	0.23	0.048	0.058	117000	120000	
	8	140	28	0	2	-0.5	0.38	0.39	0.168	0.175	46000	60000	
	8	140	28	0	2	-1.0	0.468	0.47	0.288	0.344	31100	35000	
LY-12	4	100	31	0.1	2	0	0.31		0.011		32900	32000	
	4	100	31	0.1	2	-1.0	0.416		0.151		6100	8000	
2024-T3	2.54	152	34.4	0.4	2.3	-0.9	0.474		0.246	0.230	15700	18875	(12)
	2.54	152	17.8	0.4	2.3	-1.56	0.352		0.04		34200	39850	

V. Predictions of fatigue crack growth life of structures under spectrum loadings

The loadings of aircraft structures are random in nature. Loadings spectrum used for predicting or testing always contain tensile, compressive, tensile-compressive and compressive-tensile overloadings. Based on rational assumptions, we can predict the fatigue crack growth life of structures under complex spectrum loadings by the present model. These assumptions are as follows

1. The raterdation effects of multiple overloads are larger than that of the single overload, but during the application of multiple overload the high stress level increases the crack growth rate, as a result it's effect on the total life of structure is very little[7], so the multiple overloads may be taken as a loading block (program block), it's retardation effect may be predicted just as a single overload is applied.

2. Compressive-tensile overload case may be predicted as the tensile overload case.

3. When the overload ratio $r < 1.3$, the retardation may be not token into account since it's effect is very little.

4. When there is only a compressive load in the spectrum loading, it's influence may be considered negligible.

In this paper, the fatigue crack growth life of a swivel arm of aircraft landing gear under complex spectrum loadings is calculated.

In each landing of aircraft, landing impact, running impact, taxing turn, nose wheel static control, nose wheel oscillation, peak pressure braking, normal pressure braking may be taken place. Loading spectrums are very complex.

The material used for the swivel arm of landing gear is 30 CrMnSiA, crack is surface semi-elliptic crack. Applying the given loads continuosly, as the effective crack size is growing up to be equal to the thickness of the arm wall, it may be considered that the critical crack size is reached, in that time, the number of loading cycles is the fatigue crack growth life. Predictions agree fairly well with reference (8).

In this paper, the fatigue crack growth lifes of stiffened sheets of some transport aircraft wing under spectrum loadings are predicted too. Baseline cyclic loadings are $(1\pm0.3)g$, ultimate loadings are $(1\pm0.8)g$, since there are maneuvering flights and gust loads. The predictions by the present method show that if the total life is estimated by simply adding the results of integration on the relation between da/dN and ΔK for each portion of the loading sequence, the fatigue life in actual structures this obtained will lead to error of significant magnitude[9].

All the above results demonstrate that the present model is applicable and simple for predicting the fatigue life of structures under spectrum loadings.

Acknowledgments

The author wishes to express his gratitude to Professor He Qing-Zhi of Beijing Institute of Aeronautics and Astronautics for suggesting this investigation as well as for his encouragement.

References

(1) Matsuoka, S. and Tanaka, K., "The Retardation Phenomenon of Fatigue Crack Growth in HT80 Steel," Eng. Fract. Mech. 1976. No.3.

(2) Huang Yu-shan, Liu Xue-hui and Ni Hui-lia "Overload Retardation Models of Fatigue Crack Growth", ACTA MECHANICA SOLIDA SINICA, 1981.2.

(3) Gu Mingda et al, "An Evaluation of Overload Models on The Retardation Behavior in A Ti-6Al-4V Alloy", Journal of Aeronautical Materials, 1981.2.

(4) Kobayashi, H., Nakamura, H., Hirano, A., Nakazwa, H., "A Fractographic Approch to the Influence of a Single Peak Overload on Fatigue Crack Growth", Proceedings of Fatigue'81. March 1981.

(5) Miyamoto, H., Elastic-Plastic Fracture Mechanics, Chap.2, Beijing Institute of Aeronautics and Astronautics Press (1980).

(6) Ogura, K., Ohji, K., Honda, K., "Influence of Micanical Factors on the Fatigue Crack Closure", Fracture 1977, Vol.2, ICF-4.

(7) Trebules, V.W., Roberts, Jr., R., Hertzberg, R.W., "Effect of Multiple Overloads on Fatigue Crack Propagation in 2024-T3 Aluminum Alloy" ASTM STP 536.

(8) Yang Bian-Xing, "The Predictions of Crack Growth Life in Aircraft Landing Gear" Technique Report of Beijing Institute of Aeronautics and Astronautics, 1979.3.

(9) BIAA et al, "Fracture Analysis of Stiffened Sheets", Proceedings, Second National Conference on Fracture Mechanics, Beijing, China, 1977.

(10) Matsuoka, S., Tanaka, K., "Delayed Retardation Phenomena of Fatigue Crack Growth in Various Steels and Alloys", J. Mat. Sci 13 1978, 1335.

(11) Mills, W.J., Hertzberg, R.W., "Load Interaction Effects on Fatigue Crack Propagation in 2024-T3 Aluminum Alloy", Eng. Fract. Mech. 1976.4.

(12) Crandall, G.M. and Hillberry, B.M., "Effect of Stress Level on Fatigue Crack Delay Behavior", Fracture 1977. Vol.2. ICF4.